CHARA Technical Report

No. 98 28 May 2019

Using the Mean Power Spectrum to Compute the Visibility with REDFLUOR

G. H. Schaefer

ABSTRACT: An option has been added to the `redfluor` reduction pipeline to compute the visibility from the mean power spectrum rather than taking the mean of the visibilities computed from the individual scans. This can improve the noise subtraction, particularly for low S/N data. This technical report describes the procedure used to compute the mean power spectrum and the bootstrap technique used to compute the uncertainties. It also explains additional flags added to the software and provides examples of how to use these new features.

1. INTRODUCTION

`Redfluor` is the main reduction pipeline for CLASSIC and JOUFLU data. Over the last few years changes have been made to the code in an attempt to improve the reduction of low S/N fringes. One of these changes was implemented in February 2018 and uses a weighted mean of the visibilities computed from the individual scans. The fringe weights are computed from a ratio of the power on and off of the fringes. The option to use the weighted mean is `ON` by default and can be turned `OFF` using the `-M` flag.

Another modification was implemented in February 2019 to prevent negative visibilities from being produced by background subtraction of low S/N data. This option uses the mean power spectrum of the noise scaled to the low frequency region of the fringe power spectra of each individual scan. It is `ON` by default and can be turned `OFF` using the `-Z` flag. While minimizing the likelihood of negative visibilities, this option sometimes yields systematic differences in the calibrated visibilities derived for both high and low S/N data.

The most recent modification was added in May 2019 and computes the visibility from the mean power spectrum which will have higher signal than the power spectra of the individual scans. This method is described in more detail below.

2. COMPUTING THE MEAN POWER SPECTRUM

The subroutine `process_scan` is used to normalize the fringe signal and compute the power spectrum of each individual scan. The fringe weights are used to compute the weighted mean power spectrum of all scans.

[1]Center for High Angular Resolution Astronomy, Georgia State University, Atlanta GA 30303-3083
Tel: (404) 651-2932, FAX: (404) 651-1389, Anonymous ftp: chara.gsu.edu, WWW: http://chara.gsu.edu

The mean power spectrum of the noise is computed in one of two ways. If the off-fringe frames are present and used, then the off-fringe signals are extracted to contain the same number of samples as used in the data scans (set by the envelope size and multiplier), and are centered in the middle of the scan (rather than by the position of the fringe envelope as is done in the data scans). The `process_scan` subroutine is used to normalize the extracted off-fringe signals and compute the power spectrum of individual off-fringe scans. The mean power spectrum of the noise is then computed from the off-fringe data.

If the off-fringe data is not present or is not being used, then the noise is computed from the shutters. The mean power spectra (without normalization) is computed for shutter A, shutter B, and the dark sequences. The noise power spectrum is then computed from MEAN_PS_SHUTTER_A + MEAN_PS_SHUTTER_B − MEAN_PS_DARK over the full length of the scan.

The mean noise power spectrum is scaled to the mean fringe power spectrum using the mean ratio computed from two bands of ± 20 Hz on either side of the power spectrum integration window. Frequencies below the DC suppression (set by the `-U` flag) are not included when computing the scaling factor. The fringe and scaled noise power spectra are smoothed (if requested) and then subtracted.

Errors in the noise subtraction are corrected by computing a linear fit to the noise-subtracted mean power spectrum on either side of the fringe integration window. The excess noise is sampled in a region size set by 50% of the fringe integration width on either side of the integration window. Again, frequencies below the DC suppression (set by the `-U` flag) are not included. A linear fit is computed for the excess noise and subtracted from the mean power spectrum. Because the linear fit is calculated based on frequencies closest to the fringe peak, the fit may over-estimate or under-estimate the excess noise at the ends of the scan. To minimize the impact, the subtraction of the linear fit is tapered for frequencies outside of the region used to compute the excess noise.

The visibility of the final noise-subtracted mean power spectrum is calculated by integrating the fringe power across the integration window. Uncertainties in the visibility are computed through a bootstrap approach. The subroutine `calculate_mean_ps_bootstrap` computes 1000 bootstrap iterations. During each iteration, data scans are selected at random (with replacement) to compute a new array of data scans. This randomly sampled data set is processed using the same procedure as the original data set, and the visibility is computed from the mean power spectrum. After the 1000 bootstrap iterations are complete, the standard deviation of the bootstrapped visibility distribution is adopted as the uncertainty.

The visibility from the mean power spectrum and the bootstrap uncertainties are saved to the `.info` file and printed to the screen using the `V2_MEAN_PS` keyword. As with the other visibility estimators, a value is given for signal 1, signal 2, and the difference signal. If the display flag `-d` is greater than 0, then the mean signal power spectra, the mean noise spectra, and the noise-subtracted mean power spectra will be plotted as shown in Figure 1.

When the V2_MEAN_PS visibility estimator is selected during the `calibir` calibration procedure, then the `-n` flag in `calibir` that toggles using the standard error rather than the standard deviation is automatically turned off and the `stderr_stddev` variable is set to `FALSE`. This is because the uncertainty in V2_MEAN_PS is determined from the standard deviation of the bootstrap distribution, so it would be incorrect to divide by the `sqrt` of the number of scans.

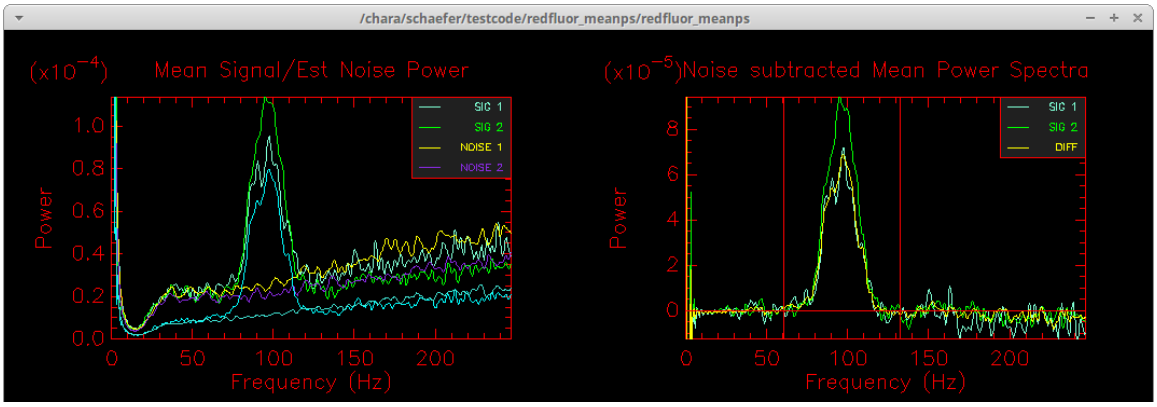

FIGURE 1. *Left:* Mean power spectra for Signal 1, Signal 2, and the Difference Signal. Overplotted are the mean noise power spectra computed from the off-fringe scans. The noise power spectra have been scaled by the mean ratio of the signal power to the noise power in two-bands of 20 Hz surrounding the fringe integration window. *Right:* Noise-subtracted mean power spectra for Signal 1, Signal 2, and the Difference Signal. The correction to remove any excess linear slope after the noise subtraction was applied by computing a linear fit to frequencies within 50% of the integration width on either side of the fringe window. The DC suppression frequency was set to 30 Hz using the `-U30` flag so that frequencies below this limit were not included in the scaling of the noise or removing any excess linear slope in the background.

3. EXAMPLES OF HOW TO USE THE MEAN POWER SPECTRUM VISIBILITY ESTIMATOR

There are two flags in `redfluor` related to computing the visibility from the mean power spectrum:

```
-m    Toggle compute V2 from weighted mean power spectrum (ON)
-N    Toggle correct PS for linear slope after noise subtraction (ON)
```

Both are `ON` by default and can be turned off by setting the `-m` or `-N` flags.

The bootstrap loop to compute the uncertainties might take a few minutes to run. Therefore, if you are not interested in computing the visibility from the mean power spectrum, you can turn off this visibility estimator by setting the `-m` flag. The `redfluor` pipeline will then run more quickly, but it will not produce the `V2_MEAN_PS` visibility estimator.

Figure 2 shows an example of when the excess noise correction is used to flatten the background in the noise-subtracted mean power spectrum. If there are noise peaks in the power spectrum near the fringe integration window, then this could corrupt the linear fit to correct for any excess noise. Figure 3 shows an example of this. In situations like this, the linear slope correction can be turned off by using the `-N` flag.

As a final example, Figure 4 shows an older data set where no off-fringe data were collected. In this case, the mean power spectrum of the noise is computed from the shutter sequence. Because the power spectra for the shutters are not normalized, the shape of the power spectra for the noise and the signals can be quite different at low frequencies. The `-U` flag can be used to set the DC suppression frequency so that frequencies below the limit are not included when scaling the noise power spectrum.

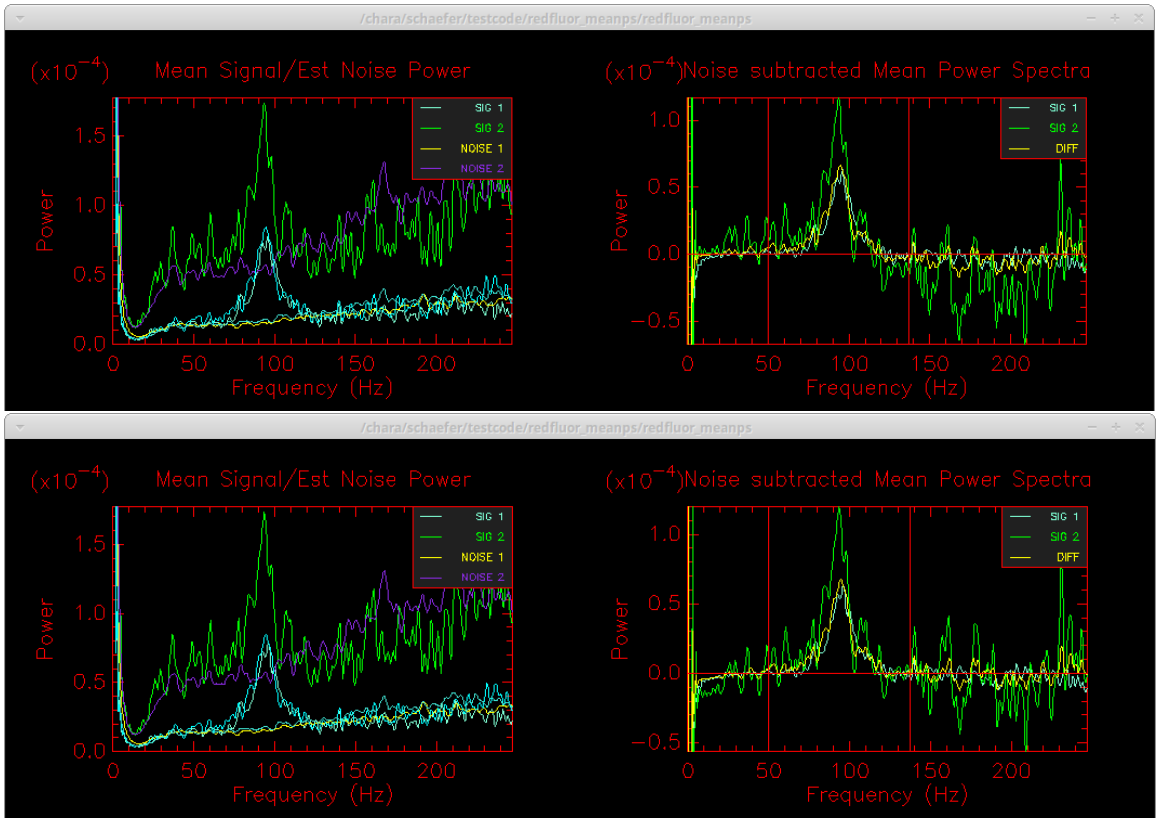

FIGURE 2. Example of the excess noise correction. The top row shows an example of the results for the mean power spectrum for low S/N data when the linear excess noise correction is turned off using the `-N` flag. There is a residual slope in the background of the noise-subtracted mean power spectra on either side of the integration window. The bottom row shows the results by including the linear excess noise correction. The noise-subtracted mean power spectra are now centered around zero on either side of the integration window. The DC suppression frequency was set to 30 Hz using the `-U30` flag so that frequencies below this limit were not included in the scaling of the noise or excess noise correction.

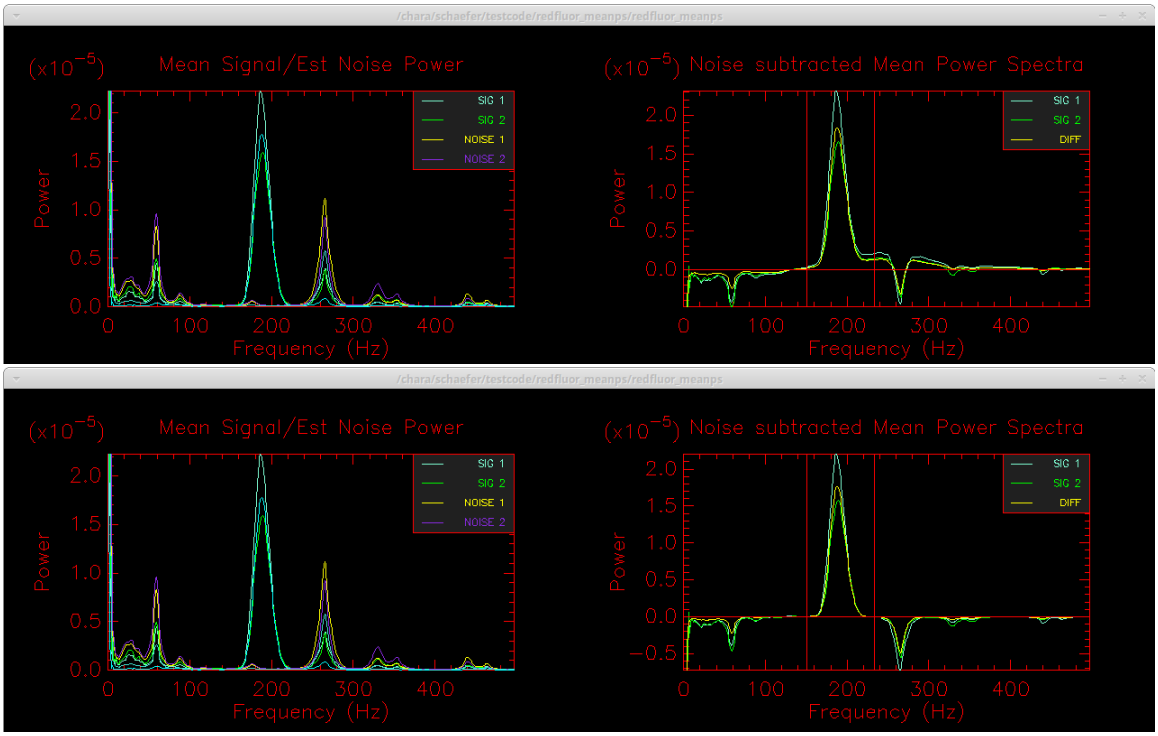

FIGURE 3. Example of a problem with the excess noise correction. The top row shows an example of the results when large noise spikes are in the power spectrum. This corrupts the linear fit to correct for excess noise on either side of the integration window. The bottom row shows that the results are improved significantly by setting the `-N` flag to turn off the excess noise correction.

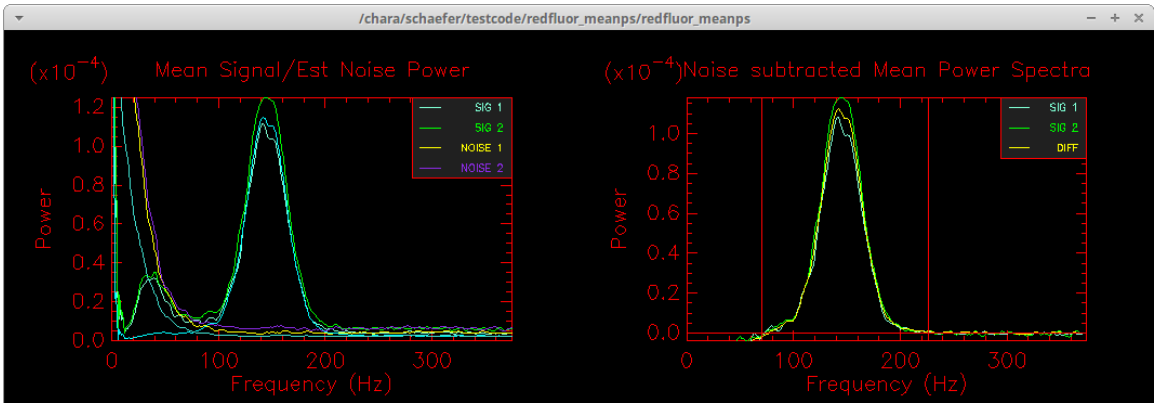

FIGURE 4. Example of an older data set where no off-fringe data were collected. Therefore, the mean power spectrum of the noise is computed from the shutter sequence. Because the power spectra for the shutters are not normalized, the shape of the power spectra for the noise and the signals are different at low frequencies. The DC suppression frequency was set to 60 Hz using the `-U60` flag so that frequencies below this limit were not included in the scaling of the noise. The excess noise correction was not applied because there were too few frequencies between the DC suppression frequency and the lower bound of the integration window.

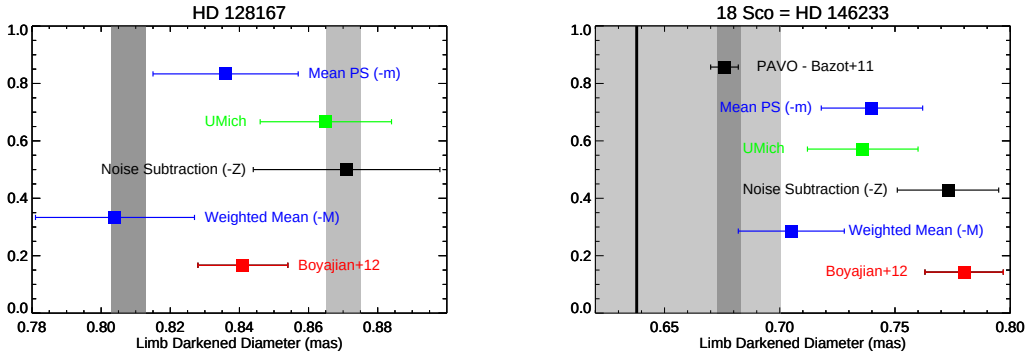

FIGURE 5. Comparison of limb-darkened angular diameters for HD 128167 (left) and HD 146233 based on Classic data using different reduction methods: reduceir (Boyajian et al. 2012), redfluor using the weighted mean of the visibilities from individual scans (`-M` toggle switch), scaling of the noise subtraction for individual scans (`-Z` toggle switch), and the visibility from the mean power spectrum (`-m` toggle switch). We also performed a reduction using John Monnier's IDL code (labeled as UMich reduction). Also plotted is the diameter for HD 146233 derived from PAVO observations (Bazot et al. 2011). The vertical dark gray band shows the limb-darkened diameter derived from the photometric effective temperature from Casagrande et al. (2011). The light gray band shows the limb-darkened diameter from the JMMC catalog (Bourgés et al. 2014). The JMMC diameter for HD 146233 extends past the plotting range, so we mark the central value with the vertical black line.

4. COMPARISON OF RESULTS

During each modification of the redfluor code described in Section 1, we have been reducing the same sets of data on HD 128167 and HD 146233 for comparison. These results are shown in Figure 5. The diameter derived from the mean power spectrum and bootstrap uncertainties overlap with most previous measurements derived from the CLASSIC data. However, offsets between the the CLASSIC diameters and the predicted value derived from Casagrande et al. (2011) and JMMC diameters still exist.

5. REFERENCES

Bazot, M., Ireland, M. J., Huber, D., et al. 2011, *A&A*, 526, L4
Bourgés, L., Lafrasse, S., Mella, G., et al. 2014, *Proc: ASPC conference on Astronomical Data Analysis Software and Systems XXIII*, 485, 223
Boyajian, T. S., McAlister, H. A., van Belle, G., et al. 2012, *ApJ*, 746, 101
Casagrande, L., Schönrich, R., Asplund, M., et al. 2011, *A&A*, 530, A138